

THE TRIGONOMETRIC WAVELET FINITE ELEMENT METHOD APPLIED TO FREE VIBRATION ANALYSIS OF EULER-BERNOULLI BEAMS

Thamara Petroli

thamarapetroli@gmail.com

Marcos Arndt

arndt@ufpr.br

Roberto Dalledone Machado

rdm@ufpr.br

*Graduate Program in Numerical Methods in Engineering, Federal University of Paraná
Curitiba, 81.531-980, Paraná, Brazil*

Abstract. Over the past years several numerical methods have been formulated so as to not only find the numerical solution of a mathematical model that describes a phenomenon, but also to find this solution in the fastest way, with low computational cost and especially, in the most accurate way. One of the characteristics of the enriched methods based on the Finite Element Method (FEM) is the possibility of including new shape functions, which are not necessarily polynomial, in the approximate solution space. The Wavelet Finite Element Method (WFEM) is an example of an enriched method that seeks to find numerical solutions to engineering problems using the adaptability that Wavelet functions present. The WFEM is the combination of FEM and Wavelets. WFEM uses the so-called scaling functions as shape functions, whose linear combination, using the FEM techniques, will describe the approximate solution space. In this sense, the objective of this work is to study the use of trigonometric Wavelets as enrichment functions in WFEM for dynamic analysis of structures, seeking to combine the high convergence rates of enriched methods with the trigonometric Wavelet properties. In this work the trigonometric WFEM method is applied to free vibration analysis of Euler Bernoulli beams in order to verify its efficiency in dynamic analysis. The natural frequencies obtained by the WFEM are compared with those obtained from analytical solutions and by other numerical methods such as the traditional FEM.

Keywords: Wavelets, Finite Element Method, Dynamic Analysis

1 Introduction

In numerical analysis, classical methods such as the Finite Element Method, the Finite Difference Method, the Spectral Finite Element Method and the Generalized Finite Element Method, are powerful tools for solving partial differential equations.

The Finite Element Method (FEM) is an approximate method that seeks to find the solution of differential equations from the construction of approximation spaces. Being a robust and easily accessible method, it is widely used in dynamic analysis.

Therefore, this method has become the basis of other methods such as the Generalized Finite Element Method (GFEM), proposed by Babuška et al. [1], which is a combination of FEM and the Partition of Unit Method. Another method based on FEM is the Wavelet Finite Element Method (WFEM), proposed by Ko et al. [2]. The WFEM is a numerical method developed in recent years, using wavelet functions or scale functions as interpolating functions to construct the approximated space.

As the family of wavelets is large, there are countless applications that can be found. For He and Ren [3] the advantages of wavelets are the multiresolution, localization properties and various basis functions that are suitable for the structural problems with local high gradient. Trigonometric wavelets are the simplest periodic analytic wavelets that can be used as interpolating functions. Thus the combination of trigonometric wavelets and multiresolution analysis is very advantageous [3].

The use of trigonometric wavelets was proposed by Chui and Mhaskar [4]. They constructed wavelets in terms of sine and cosine functions, using the multiresolution properties to map the space.

Inspired by this previous work, Quak [5] presented two approaches for the construction of the trigonometric scale functions: the first one selecting the mesh as a dyadic mesh and imposing the conditions of the Kronecker delta on the derivatives and functions in their extremes; and the second approach using the interpolation properties for the construction of the derivative, using the 2-scale scheme, to apply the multiresolution analysis.

The approach presented by Quak [5] inspired other works such as Gao and Jiang [6] that applies Hermitian trigonometric wavelets (which are nothing more than combination of the trigonometric wavelet functions with the Hermite polynomials) in the Galerkin method, in cases where the problem has singularities.

He and Zhu [7], He and Ren [8, 9] applied Hermitian trigonometric wavelets, as in Quak [5], playing the role of interpolation functions in the FEM and in the Composite Element Method. Even with different approaches focusing on beam and plate elements, the results were satisfactory, showing good convergence with a small number of degrees of freedom.

Inspired by He and Ren [3] this work aims to analyze how a Hermitian trigonometric WFEM behaves in dynamic analysis of Euler-Bernoulli beams. For this purpose an analysis of the frequency spectrum will be made, comparing WFEM performance with FEM performance.

2 Dynamic Analysis of Structures

The problem of free vibration of non-damped structures can be described by [10]:

$$K\phi = \omega^2 M\phi \quad (1)$$

where K is the stiffness matrix, M is the mass matrix, ω is the natural frequency and ϕ is the mode vector of natural vibration. The matrices K and M derived from Galerkin's form concerning the dynamic equilibrium of the system for Euler-Bernoulli beams, are given by:

$$K = [k_{ij}] = EI \int_{\Omega} \frac{\partial^2 \Phi_i}{\partial x^2} \frac{\partial^2 \Phi_j}{\partial x^2} d\Omega \quad (2)$$

$$M = [m_{ij}] = \rho A \int_{\Omega} \Phi_i \Phi_j d\Omega \quad (3)$$

where Φ 's are the interpolation functions, E is the Young modulus, I is the moment of inertia, A is the cross sectional area, ρ is the density and Ω the global domain of the problem.

3 Trigonometric Hermite Wavelet

Wavelets are described as a class of functions that are represented locally in both space and time.

They are used as a representation of a function base and derived from a specific function called the *mother wavelet* $\psi(x)$. For a chosen mother wavelet, one can apply translations and dilations.

$$\left\{ \psi \left(\frac{x+b}{a} \right), \quad (a, b) \in \mathbb{R} \times \mathbb{R}, a \neq 0 \right\}, \tag{4}$$

so that, it will cover the entire space if the choice of these parameters is made conveniently [11]. Quak [5] presented one-dimensional trigonometric wavelets for Hermite interpolation, where the trigonometric Hermite wavelet scale functions are defined for any $j \in \mathbb{N}$ as:

$$\varphi_{j,0}^0(x) = \begin{cases} \frac{1}{2^{2j+2}} \frac{\sin^2(2^j x)}{\sin^2\left(\frac{x}{2}\right)} & x \notin 2\pi\mathbb{Z} \\ 1 & x \in 2\pi\mathbb{Z} \end{cases} \tag{5}$$

$$\varphi_{j,0}^1(x) = \begin{cases} \frac{1}{2^{2j+2}} (1 - \cos(2^{j+1}x)) \cot\left(\frac{x}{2}\right) & x \notin 2\pi\mathbb{Z} \\ 0 & x \in 2\pi\mathbb{Z} \end{cases} \tag{6}$$

The figures 1 and 2, show the scale functions with $j = 2$.

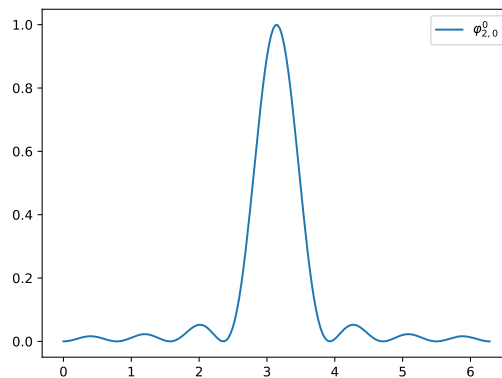


Figure 1. Scale function $\varphi_{2,0}^0$

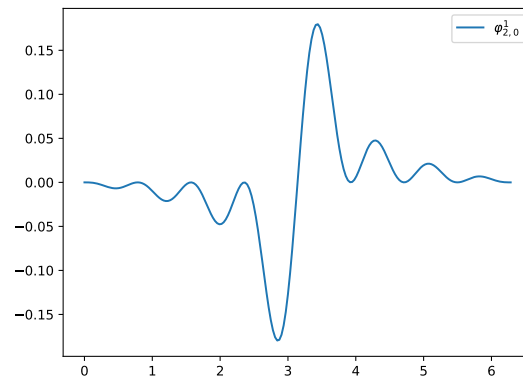


Figure 2. Scale function $\varphi_{2,0}^1$

And the corresponding trigonometric Hermite wavelet functions are given by:

$$\psi_{j,0}^0(x) = \frac{1}{2^{j+1}} \cos 2^{j+1}x + \frac{1}{3 \cdot 2^{2j+1}} \sum_{l=2^{j+1}+1}^{2^{j+2}-1} (3 \cdot 2^{j+1} - l) \cos lx \quad (7)$$

$$\psi_{j,0}^1(x) = \frac{1}{2^{2j+3}} \sin 2^{j+2}x + \frac{1}{3 \cdot 2^{2j+1}} \sum_{l=2^{j+1}+1}^{2^{j+2}-1} \sin lx \quad (8)$$

The figures 3 and 4 show the trigonometric wavelet functions with $j = 2$.

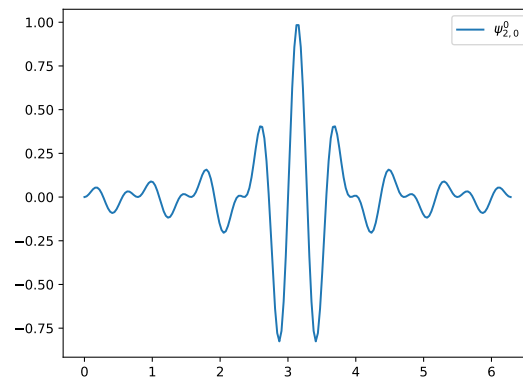


Figure 3. Wavelet function $\psi_{2,0}^0$

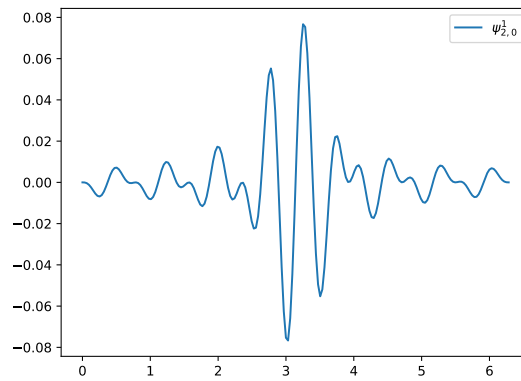


Figure 4. Wavelet function $\psi_{2,0}^1$

The nodes for the interpolation processes are equally spaced on the interval $[0, 2\pi)$ according to the step in the dyadic mesh, that is:

$$x_{j,n} = \frac{n\pi}{2^j}, \quad j \in \mathbb{N}, \quad n = 0, 1, 2, \dots, 2^{j+1} - 1 \quad (9)$$

setting φ in the dyadic mesh as:

$$\begin{aligned} \varphi_{j,n}^0(x) &= \varphi_{j,n}^0(x - x_{j,n}) \\ \varphi_{j,n}^1(x) &= \varphi_{j,n}^1(x - x_{j,n}) \end{aligned} \quad (10)$$

By satisfying the properties of Eq. (10) for each $k, n = 0, 1, 2, \dots, 2^{j+1} - 1$ one obtains:

$$\begin{aligned} \varphi_{j,n}^0(x_{j,k}) &= \delta_{k,n}, \quad \left(\varphi_{j,n}^0(x_{j,k})\right)' = 0 \\ \varphi_{j,n}^1(x_{j,k}) &= 0, \quad \left(\varphi_{j,n}^1(x_{j,k})\right)' = \delta_{k,n} \end{aligned} \quad (11)$$

$$\begin{aligned} \psi_{j,n}^0(x_{j,k}) &= \delta_{k,n}, \quad \left(\psi_{j,n}^0(x_{j,k})\right)' = 0 \\ \psi_{j,n}^1(x_{j,k}) &= 0, \quad \left(\psi_{j,n}^1(x_{j,k})\right)' = \delta_{k,n} \end{aligned} \quad (12)$$

where $(\cdot)'$ denotes the derivative of the function and

$$\delta_{k,n} = \begin{cases} 1, & k = n \\ 0, & k \neq n \end{cases} \quad (13)$$

The space of the scale functions in $L^2(0, 2\pi)$, given by its translations Eq. (10), presents properties of the multiresolution analysis with trigonometric functions, that is, this space is formed by a measurable collection of functions defined in the interval $(0, 2\pi)$. Thus we can define the space of the scale functions as:

$$V_j = \text{span} \{ \varphi_{j,n}^0, \varphi_{j,n}^1 : n = 0, 1, 2, \dots, 2^j - 1 \} \quad (14)$$

$$= \{ 1, \cos x, \dots, \cos(2^{j+1} - 1)x, \sin x, \dots, \sin 2^{j+1}x \} \quad (15)$$

And by multiresolution, the orthogonal complement space of V_j relative to V_{j+1} , is the space formed by the wavelet functions denoted by W_j , and defined as:

$$W_j = \text{span} \{ \psi_{j,n}^0, \psi_{j,n}^1 : n = 0, 1, 2, \dots, 2^{j+1} - 1 \} \quad (16)$$

$$= \{ \cos 2^{j+1}x, \dots, \cos(2^{j+2} - 1)x, \sin(2^{j+1} + 1)x, \dots, \sin 2^{j+2}x \} \quad (17)$$

3.1 Adaptive Interpolation

He and Ren [3] present a set of functions based on the trigonometric wavelets, with scale $j = 1$, to be appointed as shape functions in the Wavelet Finite Element Method (WFEM).

The set of scale functions, which were obtained through a modification in the translation of the scale functions of the Equations 5 and 6, with multiresolution level $j = 1$, are defined as (Fig. 5) [3]:

$$\begin{cases} \varphi_{1,m}^0 = \cos^2(x - m)\pi \cos^2 \frac{(x - m)\pi}{2} \\ \varphi_{1,m}^1 = \sin(x - m)\pi \cos^2(x - m)\pi \cos^2 \frac{(x - m)\pi}{2} \end{cases} \quad (m = 0, 0.5, 1, 1.5; 0 \leq x \leq 1) \quad (18)$$

The functions $\varphi_{1,m}^n$ ($m = 0, 0.5, 1, 1.5; n = 0, 1$) have the properties:

$$\varphi_{1,m}^n(0) = \begin{cases} 1, & \text{if } n = 0, m = 0 \text{ ou } m = 1 \\ 0, & \text{otherwise} \end{cases} \quad (19)$$

$$(\varphi_{1,m}^n(0))' = \begin{cases} 1, & \text{if } n = 1, m = 0 \text{ ou } m = 1 \\ 0, & \text{otherwise} \end{cases} \quad (20)$$

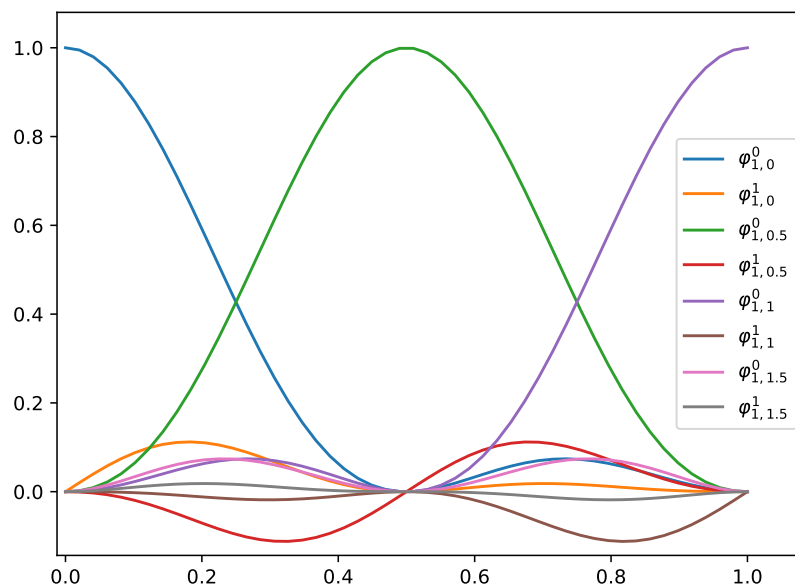


Figure 5. Adaptive Trigonometric Wavelet Functions

Defined in the interval $[0, 1]$, this set of functions presents the characteristics of good approximation presented by the trigonometric functions of Hermite and the characteristic of multiresolution, local characteristic of the wavelets.

Due to the interpolation properties of the trigonometric Hermite wavelets, the boundary conditions and the connection between the adjacent elements can be processed in a conventional manner, without the need to introduce an additional transformation matrix that connects the element parameters to the wavelet coefficients. Moreover, the trigonometric wavelets make the best use of the high accuracy of the trigonometric series, due to the multiresolution tool.

Assuming that the element is a three-node beam element, the displacement field is expressed as:

$$w = \sum_{i=1}^8 a_i \varphi_i(\xi) = \Phi \{a\} \tag{21}$$

where $\xi \in [0, 1]$ denotes the local coordinate, and

$$\Phi = \left[\varphi_{1,0}^0 \quad \varphi_{1,0}^1 \quad \varphi_{1,0.5}^0 \quad \varphi_{1,0.5}^1 \quad \varphi_{1,1.5}^0 \quad \varphi_{1,1.5}^1 \quad \varphi_{1,1}^0 \quad \varphi_{1,1}^1 \right] \tag{22}$$

$\{a\}$ contains the coefficients to be determined (degrees of freedom), in the form:

$$\{a\} = \left[u_1 \quad u'_1 \quad u_2 \quad u'_2 \quad a_5 \quad a_6 \quad u_3 \quad u'_3 \right] \tag{23}$$

where u_1, u_2 and u_3 are the nodal displacements, u'_1, u'_2 and u'_3 are the nodal rotations and, a_5 and a_6 are the field degrees of freedom (non nodal), those that have no physical meaning.

The stiffness and mass matrices are defined as in MEF by Eq. (2) and Eq. (3).

4 Numerical Results

In order to evaluate the efficiency of the trigonometric WFEM, it was considered an Euler-Bernoulli beam in two cases: a clamped-free beam (Fig. 6) and a simply supported beam (Fig. 8). The results obtained using the WFEM were compared to those obtained by FEM using 3 elements and the trigonometric approach of the Generalized Finite Element Method (GFEM), as presented in [12], using 1 element and 2 levels of enrichment in order to use the same number of degrees of freedom.

4.1 Clamped-free beam

For comparison purposes, the beam has unit size $L = 1$.

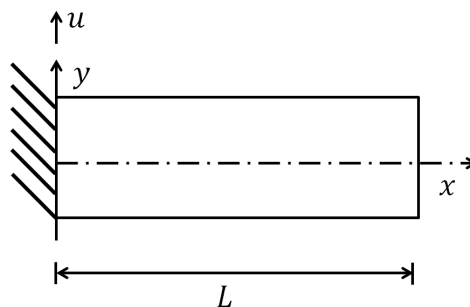


Figure 6. Clamped-free beam

The natural analytic frequencies (ω_r) are obtained by the solution of the frequency equation in the classical form:

$$\cos(\kappa_r L) \cosh(\kappa_r L) + 1 = 0 \quad r = 1, 2, \dots \quad (24)$$

$$\kappa_r = \left(\frac{\omega_r^2 \rho A}{EI} \right)^{\frac{1}{4}} \quad (25)$$

The analytical dimensionless eigenvalues ($\chi_r = \kappa_r L$) and those obtained by FEM (3 elements), GFEM (1 element and 2 levels of enrichment) and WFEM (1 element) are presented in Table 1.

Table 1. Eigenvalues of the clamped-free beam

r	Analytic ¹	FEM - 6 DOF	WFEM - 6 DOF	GFEM - 6 DOF
1	1.875104	1.875199	1.876902	1.875138
2	4.694091	4.701793	4.697806	4.695443
3	7.854757	7.903542	7.858735	7.880210
4	10.99554	11.86048	11.02735	11.016307
5	14.13717	16.27093	14.17883	14.158541
6	17.27876	22.97381	25.57236	17.410848

¹ Arndt [12].

It is possible to observe that only the last dimensionless eigenvalue is not close to the analytic response. Such behavior can also be analyzed through the graph of the frequency spectrum, showed in Fig. 7.

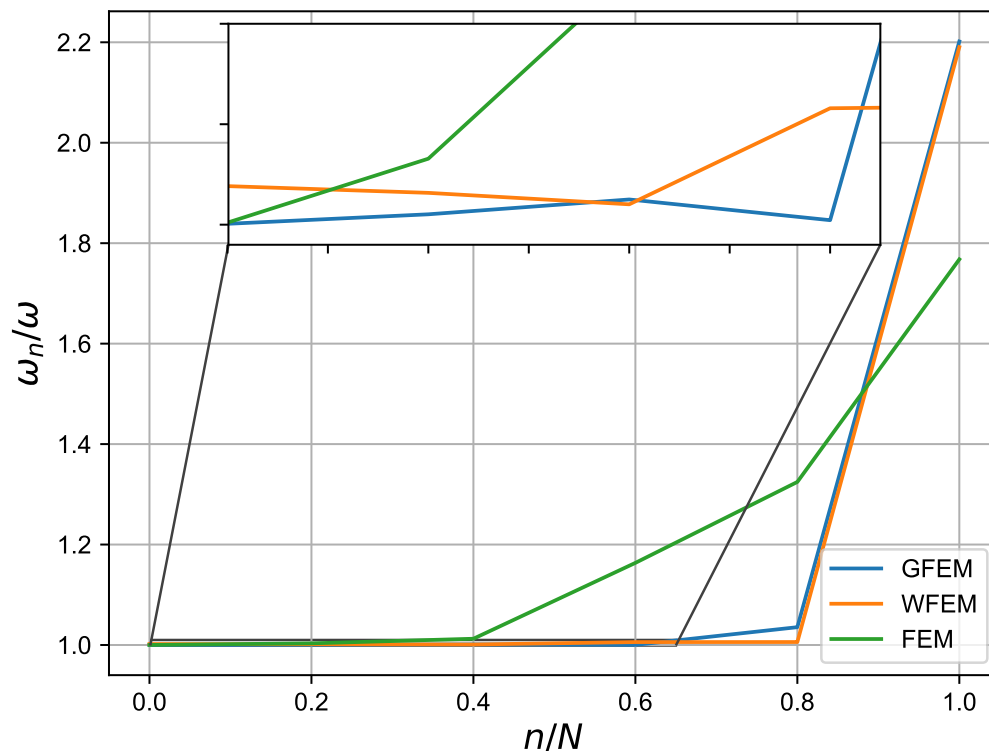


Figure 7. Clamped-free beam frequency spectrum

It can be observed that the beginning of the FEM, GFEM and WFEM spectrum is very similar. A zoom in the Fig. 7 was given in order to better observe this behavior. Observing the graph of the frequency spectrum it is possible to notice that the WFEM presents a better performance only than the FEM, however at the end of the graph in Fig. 7 the WFEM shows results worse than the GFEM.

4.2 Simply supported beam

As previously stated, the beam has a unity length $L = 1$.

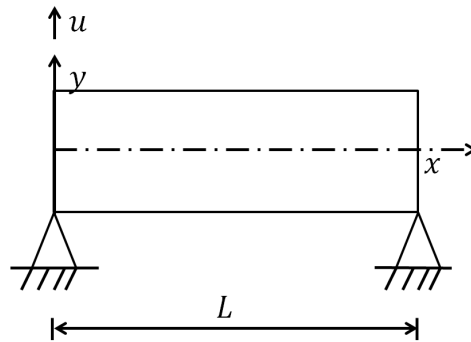


Figure 8. Simple Supported beam

The natural analytic frequencies (ω_r) obtained by the solution of the frequency equation are:

$$\kappa_r = \frac{r\pi}{L} \quad r = 1, 2, \dots \quad (26)$$

$$\kappa_r = \left(\frac{\omega_r^2 \rho A}{EI} \right)^{\frac{1}{4}} \quad (27)$$

As in the previous case the dimensionless WFEM (1 element) eigenvalues ($\chi_r = \kappa_r L$) presented in Table 2 are compared to the analytical, to the FEM (3 elements) and GFEM (1 element and 2 levels of enrichment) responses.

Table 2. Eigenvalues of the simple supported beam

r	Analytic	FEM - 6 DOF	WFEM - 6 DOF	GFEM - 6 DOF
1	3.141592	3.142864	3.015588	3.142283
2	6.283185	6.320210	6.834799	6.283284
3	9.424777	9.929252	9.013347	9.434429
4	12.566370	13.53960	13.33643	12.601550
5	15.707963	18.11118	19.75921	18.533003
6	18.849555	21.25550	26.27953	25.718526

The frequency spectrum behavior can be analyzed through the graph in Fig. 9:

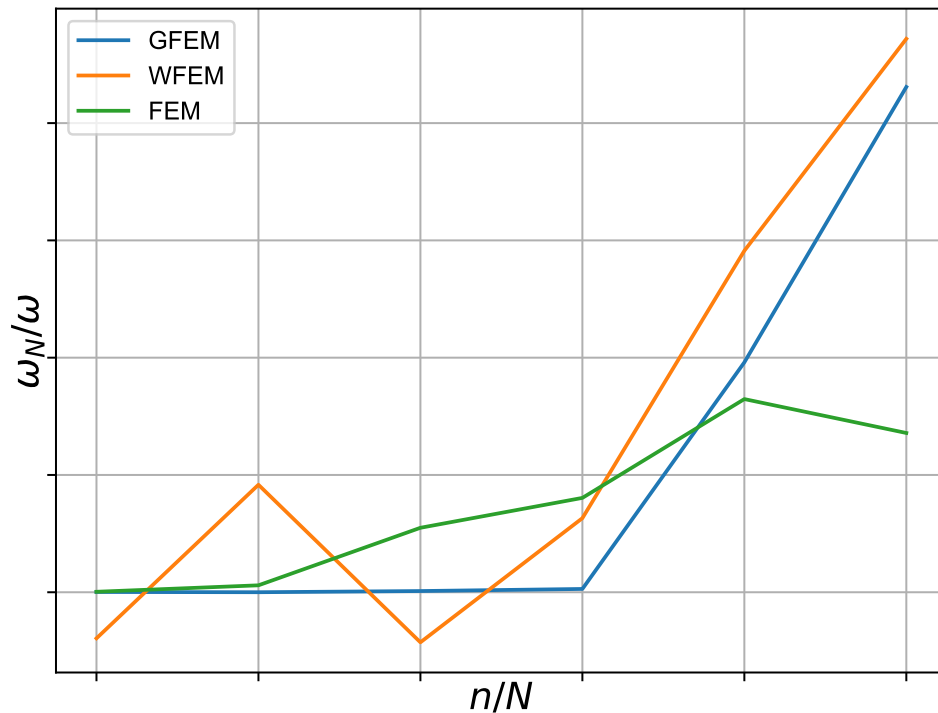


Figure 9. Simple supported beam frequency spectrum

In this example it may be noted that the WFEM don't have the best behavior, showing that in this case GFEM is better than WFEM.

5 Conclusion

This work presents the dynamic analysis of the Wavelet Finite Element Method (WFEM). The WFEM joins the Finite Element Method (FEM) and wavelet functions. As already seen, such a method inherits the properties of wavelets, such as multiresolution.

Based on the adaptive formulation presented by He and Ren [3] a frequency spectrum analysis was performed for the cases of a clamped-free beam and simply supported beam, and the results were compared with the FEM and the trigonometric approach of the Generalized Finite Element Method (GFEM), as presented in Arndt [12].

Through the graphical analysis on the clamped-free beam, it was possible to conclude that the WFEM presents a good approximation and better performance for the first frequencies. But at the end of the spectrum there was a certain divergence in the results. About the case of the simply supported beam, the behavior wasn't satisfactory, showing that GFEM presents the best results. However it is worth noting that, 3 elements were used in the FEM analysis against a single element in the WFEM analysis. As the formulation is simple this is a valid method, in the sense that it is possible to exploit it better applying the multiresolution in order to increase the precision, for example.

Acknowledgements

The authors respectfully acknowledged Capes and Araucária Foundation for the financial support.

References

- [1] Babuška, I., Banerjee, U., & Osborn, J. E., 2004. Generalized finite element methods: main ideas, results and perspective. *International Journal of Computational Methods*, vol. 1, n. 1, pp. 67–103.
- [2] Ko, J., Kurdila, A. J., & Pilant, M. S., 1995. A class of finite element methods based on orthonormal, compactly supported wavelets. *Computational Mechanics*, vol. 16, n. 4, pp. 235–244.
- [3] He, W. Y. & Ren, W. X., 2012. Finite element analysis of beam structures based on trigonometric wavelet. *Finite Elements in Analysis and Design*, vol. 51, pp. 59–66.
- [4] Chui, C. & Mhaskar, H. N., 1993. On trigonometric wavelets. *Constructive Approximation*, vol. 9, n. 2-3, pp. 167–190.
- [5] Quak, E., 1996. Trigonometric wavelets for hermite interpolation. *Mathematics of Computation of the American Mathematical Society*, vol. 65, n. 214, pp. 683–722.
- [6] Gao, J. & Jiang, Y. L., 2008. Trigonometric hermite wavelet approximation for the integral equations of second kind with weakly singular kernel. *Journal of Computational and Applied Mathematics*, vol. 215, n. 1, pp. 242–259.
- [7] He, W. Y. & Zhu, S., 2013. Progressive damage detection based on multi-scale wavelet finite element model : numerical study. *Computers and Structures*, vol. 125, pp. 177–186.
- [8] He, W. Y. & Ren, W. X., 2013a. Trigonometric wavelet-based method for elastic thin plate analysis. *Applied Mathematical Modelling*, vol. 37, pp. 1607–1617.
- [9] He, W. Y. & Ren, W. X., 2013b. Adaptive trigonometric wavelet composite beam element method. *Advances in Structural Engineering*, vol. 16, pp. 1899–1910.
- [10] Chopra, A., 2012. *Dynamics of Structures: Theory and Applications to Earthquake Engineering*. Civil Engineering and Engineering Mechanics Series. Prentice Hall.
- [11] Vidakovic, B. & Mueller, P., 1991. Wavelets for kids: A tutorial introduction. *Biometrika*, vol. 97, n. 2, pp. 435–446.
- [12] Arndt, M., 2009. *O Método dos Elementos Finitos Generalizados Aplicado à Análise de Vibrações Livres de Estruturas Reticuladas*. PhD thesis, Universidade Federal do Paraná.